VOL. 196, NO. 2 THE AMERICAN NATURALIST AUGUST 2020

# Selection and Constraints in the Ecomorphological Adaptive Evolution of the Skull of Living Canidae (Carnivora, Mammalia)

**Fabio Andrade Machado***

División Mastozoología, Museo Argentino de Ciencias Naturales "Bernardino Rivadavia"–Consejo Nacional de Investigaciones Científicas y Técnicas, Avenida Ángel Gallardo 470, C1405DJR, Buenos Aires, Argentina; and Department of Biology, University of Massachusetts, Boston, Massachusetts 02125

*Submitted February 21, 2019; Accepted March 9, 2020; Electronically published June 22, 2020*

*Online enhancements:* appendix, supplemental PDF. *Dryad data:* https://doi.org/10.5061/dryad.m63xsj3z9.

ABSTRACT: The association between phenotype and ecology is essential for understanding the environmental drivers of morphological evolution. This is a particularly challenging task when dealing with complex traits, such as the skull, where multiple selective pressures are at play and evolution might be constrained by ontogenetic and genetic factors. I integrate morphometric tools, comparative methods, and quantitative genetics to investigate how ontogenetic constraints and selection might have interacted during the evolution of the skull in extant Canidae. The results confirm that the evolution of cranial morphology was largely adaptive and molded by changes in diet composition. While the investigation of the adaptive landscape reveals two main selective lines of least resistance (one associated with size and one associated with functional shape features), rates of evolution along size were higher than those found for shape dimensions, suggesting the influence of constraints on morphological evolution. Structural modeling analyses revealed that size, which is the line of most genetic/phenotypic variation, might have acted as a constraint, negatively impacting dietary evolution. Constraints might have been overcome in the case of selection for the consumption of large prey by associating strong selection along both size and shape directions. The results obtained here show that microevolutionary constraints may have played a role in shaping macroevolutionary patterns of morphological evolution.

*Keywords:* morphometrics, natural selection, selection gradients, **G** matrix, constraints, lines of least resistance.

## Introduction

Ecomorphology has long been recognized as central to the understanding of organismic biology. The study of the relationship between morphology and ecology allows one not only to infer function from phenotypic data but also to understand the origins and evolution of key innovations, shedding light on macroevolutionary dynamics (Balisi et al. 2018; Phillips et al. 2018; Piras et al. 2018). Studying ecomorphology is particularly challenging in the case of complex phenotypes involved in a wide array of functions, such as the mammalian skull. The skull is formed by a highly conserved number of anatomical elements (Schoch 2006; Esteve-Altava et al. 2012; Koyabu et al. 2012), whose differential growth and tissue interactions determine the final configuration (Hallgrímsson et al. 2009). Variation of the skull anatomy correlates to diverse aspects of mammalian biology, such as foraging behavior (Spencer 1998; Nogueira et al. 2009; Therrien et al. 2016), perception (Heesy 2008; Finarelli and Goswami 2009; Pilatti and Astúa 2017), and cognition (Finarelli and Flynn 2009; Finarelli 2010), making the study of skull morphology a valuable tool for understanding mammalian ecology and evolution.

Studies of form-function association in skull anatomy are particularly plentiful for the family Canidae (Carnivora). Despite being highly morphologically conserved in comparison to other carnivores (Werdelin and Wesley-Hunt 2014; Michaud et al. 2018), Canidae shows a wide variation in dietary ecology ranging from generalist omnivores and insectivores to specialized carnivorous forms. Differences in diet are thought to correlate with various aspects of skull form (e.g., Werdelin 1989; Van Valkenburgh 1991; Van Valkenburgh and Koepfli 1993; Zurano et al. 2017), suggesting that a significant amount of morphological variation in the group was adaptive and can be traced back to functional causes. Specifically, a great deal of attention has been directed to morphological adaptations related to subduing and consuming large vertebrate taxa (mostly ungulates). These large-mammal specialist predators tend to be larger than omnivores and show a suite of modifications, such as a longer carnassial blade and shorter facial length, features associated with increased bite force and biomechanical performance (Slater

* Email: macfabio@gmail.com.
**ORCIDs:** Machado, https://orcid.org/0000-0002-0215-9926.

Am. Nat. 2020. Vol. 196, pp. 000–000. 
DOI: 10.1086/709610

et al. 2009; Damasceno et al. 2013; Meloro et al. 2014). While the association between large prey consumption and size is thought to be mostly indirect (i.e., through the action of metabolic constraints; Carbone et al. 2007; Tucker et al. 2016), size can be under selection to increase predatorial performance, since it correlates with biomechanical traits, such as absolute bite forces (Greaves 1983; Damasceno et al. 2013; Penrose et al. 2016).

Alternatively, because size usually corresponds to the line of maximum genetic variance in mammals ($g_{max}$), it could bias evolution by acting as a line of least resistance (Schluter 1996; Marroig and Cheverud 2010). In that scenario, selection on function-related features of the skull would result in size changes not because size itself is under selection but because it is genetically associated with the targets of selection (Lande 1979). These genetic associations act by aligning the response to selection in the direction of $g_{max}$ and away from the line of greatest increase in fitness (the gradient of selection $\beta$), thus functioning as a constraint to the evolution of multivariate systems (Marroig and Cheverud 2005; Renaud et al. 2006; Blows and Walsh 2009; Marroig et al. 2009; Marroig and Cheverud 2010). Even though these constraints were originally thought to be overcome with time (Felsenstein 1988; Schluter 1996; Arnold et al. 2001), we have recently seen a plethora of results suggesting that genetic and ontogenetic constraints might affect large-scale macroevolutionary patterns (Marroig and Cheverud 2004; Firmat et al. 2014; Simon et al. 2016; De Azevedo et al. 2017; Houle et al. 2017; McGlothlin et al. 2018). This has instigated a resurgence of interest in the effect of intrinsic constraints on macroevolution (Melo et al. 2016; Jablonski 2019). Therefore, how constraints might have affected morphological adaptation is an issue that requires further attention.

Here I investigate how ontogenetic and genetic constraints embedded into skull trait covariances have affected morphological adaptations in Canidae. To do that, I first conduct an analysis of the association between skull morphology and a newly compiled catalog of canid diet, which considers not only the amount of vertebrate meat consumed but also different food sources, such as invertebrates and plant material. I then reconstruct past selective pressures and interpret general patterns in light of biomechanical demands. Last, I evaluate how these selective pressures interacted with multivariate constraints, specifically the line of least phenotypic variance $p_{max}$ as an approximation of $g_{max}$, to shape rates of dietary evolution in the family. If constraints to evolution had only a transient effect on the ecological adaptation of the group, one would expect to find no association between constraints and the rate of ecological evolution within Canidae. On the other hand, if $g_{max}$ had a long-lasting effect on the patterns of morphological evolution of the group, one would expect constraints to have a negative impact on the rate of ecological adaptation.

## Material and Methods

### *Sample*

I investigated osteological specimens from mammal collections of the following 11 institutions: Museu de Zoologia da Universidade de São Paulo (MZUSP, São Paulo), Museu Nacional (MN, Rio de Janeiro), Museu Paraense Emílio Goeldi (MPEG, Belém), Museo Argentino de Ciencias Naturales Bernardino Rivadavia (MACN, Buenos Aires), Museo de La Plata (FCNyM, La Plata), American Museum of Natural History (AMNH, New York), National Museum of Natural History of the Smithsonian Institution (USNM, Washington), Museum of Comparative Zoology (MCZ, Harvard), Field Museum (FMNH, Chicago), and Academy of Natural Sciences of Drexel University (ANSP, Philadelphia).

I measured skulls from 1,499 adult individuals (based on tooth eruption and suture closure) belonging to 39 Canidae taxa, covering almost all living species except for *Vulpes cana*. The phylogeny used for comparative analysis was based on a recent total evidence maximum parsimony analysis (Zrzavý et al. 2018). Because Zrzavý et al.'s cladogram lacks a formal dating, here I used 29 nuclear and mitochondrial genes and fossil calibrations to estimate branch lengths and divergence times for their topology (fig. 1). See the supplemental PDF (available online) for details on the molecular analysis, including model selection (table S1; tables S1–S7 are available online) and fossil calibrations (table S2). The complete list of genes used is available as part of the data deposited in the Dryad Digital Repository (https://doi.org/10.5061/dryad.m63xsj3z9; Machado 2020).

### *Morphometrics*

For morphometric analyses, I digitized 43 anatomical landmarks (nine on the midline and 17 on each side of the skull; fig. A1; figs. A1, S1–S3 are available online) with a Microscribe MLX system. Measurements were obtained as linear interlandmark distances to measure localized changes in skull form. The list of measurements was based on Machado et al. (2018) but was expanded to include the orbit and teeth regions, specifically the length of the canine and of the fourth premolar (the carnassial). Bilateral measurements were averaged between sides, producing a set of 40 measurements (table S3). All measurements were log transformed for further analyses. See Machado et al. (2018) for further details on data processing and repeatability of measurements. Table 1 summarizes the main variables used in this study, their

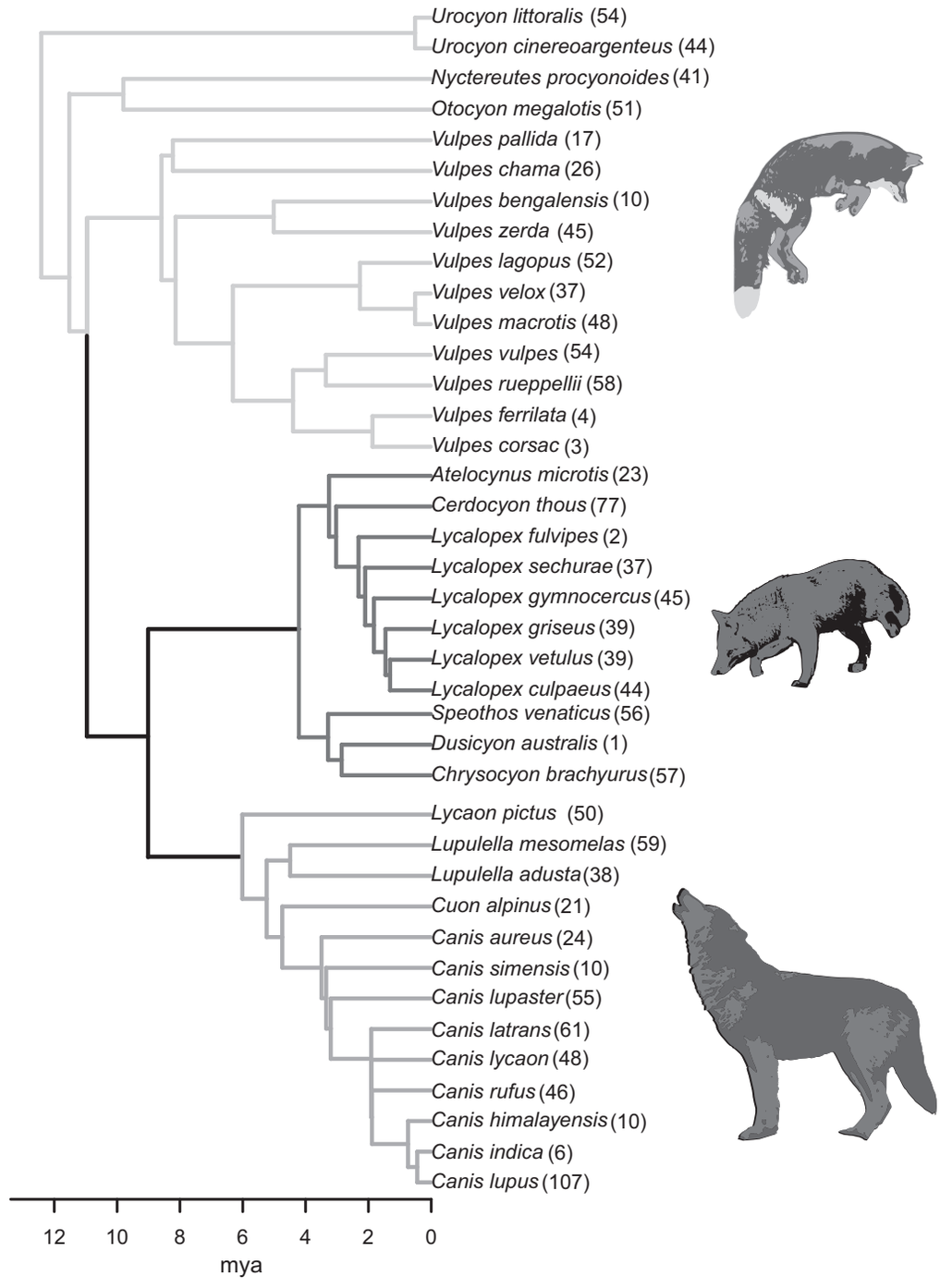


**Figure 1:** Phylogenetic hypothesis used for comparative methods. Sample sizes are shown in parentheses. Shades of gray represent the three Caninae grades: light gray = Vulpines; dark gray = Cerdocyonina; medium gray = Canina. mya = million years before present. A color version of this figure is available online.

symbols, how they were measured, and their biological interpretation.

To explore the effect of genetic constraints embedded into the covariance patterns, one needs to obtain the **G** matrix, which contains the additive genetic variance and covariance among traits (Cheverud 1984; Arnold 1992). Given that **G** is usually not available for nonmodel organisms, one common practice is to employ sample phenotypic

**Table 1:** Variables investigated in this study

| Symbol | Type | Measure | Meaning |
|---|---|---|---|
| $\mathbf{P}_w$ | Square matrix ($p \times p$) | Pooled within-group phenotypic variance-covariance matrix | Patterns and magnitude of variation and covariance among traits within a population. Used as a surrogate for the covariance matrix of additive genetic effects (**G**). |
| $p_{max}$ | Vector ($p \times 1$) | First principal component of $\mathbf{P}_w$ | Linear combination of traits that explains the large portion of phenotypic variance within a group. For Canidae, this vector represents a size vector. Used as an approximation of the genetic line of most variation $g_{max}$, or the genetic line of least resistance. |
| $\Delta z$ | Vector ($p \times 1$) | Time-standardized PICs of morphological variables | Direction and amount of phenotypic change for each morphological variable. Because PICs are time standardized, entries on the vector are point estimates of rates of evolution for each trait. |
| **B** | Square matrix ($p \times p$) | Mean squares and mean cross product of the matrix of $\Delta z$ | Among-species divergence matrix. Contains rates of evolution for each trait on the diagonals and rates of coevolution on the off-diagonal. |
| $\beta$ | Vector ($p \times 1$) | $\mathbf{P}_w^{-1}\Delta z$ | Selection gradients on each morphological variable, describing the intensity and direction of selection acting upon each individual trait. |
| $\Delta d$ | Vector ($k \times 1$) | PICs of ecological variables | Direction and amount of phenotypic change for each dietary variable. See $\Delta z$ for further detail. |
| $\|\|X\|\|$ | Scalar | Norm of vector $X$ | Size of a given vector. For $\Delta z$ and $\Delta d$, it is the multivariate rate of evolution. For $\beta$, it gives the strength of selection. |
| $\Delta z_{diet}$ | Vector ($p \times 1$) | Partial regression coefficients of the nonparametric multivariate regression analysis of morphology on diet (RRPP) | Directions of the morphometric space that are more associated with changes in specific food items. |
| $\beta_{diet}$ | Vector ($p \times 1$) | $\mathbf{P}_w^{-1}\Delta z_{diet}$ | Hypothetical selection gradients necessary to generate change along the directions most associated with each food item ($\Delta z_{diet}$). |
| $\mathbf{\Omega}$ | Square matrix ($p \times p$) | Mean squares and mean cross product of the matrix of $\beta$'s | Matrix describing the distribution of adaptive peaks on the realized adaptive landscape of a lineage. |
| $\omega_i$ | Vector ($p \times 1$) | Eigenvector $i$ of $\mathbf{\Omega}$ | Linear combination of traits that gives the $i$th SLLR. |
| $\vec{\rho}(X, Y)$ | Scalar | Vector correlation (dot product) between the normalized vectors $X$ and $Y$ | Alignment of two vectors. For individual $\beta_{diet}$ and $\omega_i$, it indicates how aligned a hypothetical selection for a food item is in relation to a SLLR. |
| Constraint ($c$) | Scalar | Vector correlation between $\Delta z$ and $p_{max}$ | Measures how aligned a particular evolutionary response is in relation to the genetic line of least resistance, measuring the constraining effect that $g_{max}$ had on the evolutionary response. |
| Evolvability ($e$) | Scalar | $\beta^T\mathbf{P}_w\beta$ | Amount of variance available on the direction of $\beta$, indicating the ability of a population to respond to selection. |

Note: Shown are variables investigated in this study, their symbols, their type (matrix, vector, or scalar) and dimensionality (in parentheses), how they were measured, and their biological interpretation. $p$ = number of craniometric traits; $k$ = number of dietary items; PIC = phylogenetic independent contrast; SLLR = selective line of least resistance.

covariance matrices, or **P**, as a surrogate for **G**. This is often justified in the presence of direct or indirect evidence that **P** and **G** can be used interchangeably (Lofsvold 1986; Kohn and Atchley 1988; Roff 1995). In a previous article (Machado et al. 2018), my colleagues and I have shown that Canidae has a stable phenotypic covariance structure for cranial traits. Because **P** matrices are a sum of genetic and environmental factors, stable **P**s are more likely explained by the presence of stable **G**s (Arnold and Phillips 1999; Marroig and Cheverud 2001). This suggests not only that individual species' **P** matrices are similar to their corresponding **G**s but also that species' **G**s will behave similarly among species (Hubbe et al. 2016). Here I use this rationale to adopt **P** as a surrogate for **G** in a macroevolutionary framework (Turelli 1988).

**P** was obtained by calculating the residuals of a linear model controlling for nuisance factors, such as subspecies and sex (table S4). Residuals obtained from all species were then pooled together, and a single within-group phenotypic covariance matrix, or $\mathbf{P}_w$, was calculated for the full sample to produce more reliable covariance estimates (Lofsvold 1986; Cheverud 1988). This assumes not only the interchangeability of $\mathbf{P}_w$ and **G** but also that **P** matrices (and therefore **G**) are relatively stable throughout the evolution of the group. $\mathbf{P}_w$ was subjected to a principal component analysis (PCA), and the first eigenvector of $\mathbf{P}_w$, or $p_{max}$, is taken as an approximation of $g_{max}$ (Marroig et al. 2009). To evaluate whether $p_{max}$ relates to size or nonsize (shape) variation, I calculated the vector correlation ($\vec{\rho}$) between $p_{max}$ and an isometric vector (Jolicoeur 1963).

### *Adaptive Evolution*

As a first step to test ecomorphological associations, I evaluated whether observed patterns of divergence differed from what is expected under the null hypothesis of genetic drift (Lande 1979; Lofsvold 1988). To test this, I employed the eigenvalue regression approach (Ackermann and Cheverud 2002), which is based on the expectation that, in the absence of natural selection, among-species divergence will be proportional to the pattern of additive genetic covariation as follows:

$$\mathbf{B} = \frac{t}{N_e}\mathbf{G}, \tag{1}$$

where **B** is the among-species divergence matrix, $t$ is time in generations, and $N_e$ is the effective population size (Lande 1979). Ackermann and Cheverud (2002) have shown that equation (1) can be rewritten in log scale and that the proportionality between **B** and **G** can be evaluated as follows:

$$\log(\text{var}_B) = a + b[\log(\lambda)], \tag{2}$$

where $\lambda$ are the eigenvalues of **G** ($\mathbf{P}_w$ in the current case), $\text{var}_B$ are the variances of **B** projected onto the eigenvectors of **G**, $a = \log(t/N_e)$, and the slope parameter $b$ is the proportionality factor among matrices. Equation (2) establishes the rates of evolution at each PC ($\text{var}_B$) as a function of the amount of available genetic/intraspecific variance at those same PCs ($\lambda$). If no selection occurred, rates of evolution will be proportional to within-group variances, and $b = 1$. If $b$ is significantly different from 1, then the null hypothesis of proportionality is rejected, suggesting that drift is not enough to explain the observed pattern of morphological evolution (for more details, see Ackermann and Cheverud 2002; Marroig and Cheverud 2004).

**B** was calculated in a phylogenetic context by obtaining time-standardized phylogenetic independent contrasts (PICs) of the morphological variables and calculating the matrix of average cross products among them. **B** calculated in this way contains the expected rates of evolution (diagonals) and of coevolution (off-diagonals) of the traits under evaluation (Revell et al. 2007). To build a null distribution, I used equation (1) to simulate 10,000 rounds of multivariate drift on the phylogeny of the group. After each round, I extracted $\lambda$ and $\text{var}_B$ and calculated their respective $b$. The null hypothesis was rejected if the observed $b$ value fell outside the 95% interval for simulated values.

### *Dietary Data and Ecomorphology*

To evaluate the association between diet and morphology, I produced a diet database for all canid species. Information on diet was obtained from a literature survey focusing on descriptions that associate each food item with its relative importance for a species. The main source of information was Sillero-Zubiri et al. (2004), complemented by mammalian species accounts (Mech 1974; Bekoff 1977; Dietz 1985; Sillero-Zubiri and Gottelli 1994; Clark 2005; Clark et al. 2008; Lucherini and Luengos Vidal 2008; Dalponte 2009; Cossíos 2010; Moehlman and Hayssen 2018) and information available from the Animal Diversity Web database (Myers et al. 2018). A semantic analysis was performed following Kissling et al.'s (2014) methodology, where a list of terms was used to associate a food item with a specific rank of importance. Because the main sources are reviews and aggregates of information, only descriptions with citations that could be checked were taken into account.

Diet categories were as follows: large mammal, small mammal, bird, herptile, fish, egg, carrion, hard-bodied invertebrate, soft-bodied invertebrate, seed, fruit, root, and leaf. Rank 1 was associated with occasional food items, rank 2 with secondary food items, and rank 3 with primary food items. Items that were not present in the description received rank 0. Note that this ranking order is

inverted in relation to Kissling et al. (2014), where rank 1 is associated with primary items and rank 3 with occasional items. Ranks were inverted here in order to treat diet as an ordinal variable in nonparametric analysis. Terms such as "consists mainly," "feeds mostly," "most frequently consumed," or "almost exclusively" were considered to establish a food item as a primary food source, while terms such as "occasionally," "sometimes," "small amounts," and "supplemented by" were used to define a food item as an occasional food source. See Kissling et al. (2014) for a full list of terms associated with each rank. Those terms are general guidelines, and the context of the text was taken into account in order to rank specific food items. For example, it was common to find descriptions that said that the diet consists mainly of a list of different items ranging from vertebrate prey to invertebrates and plant material. In those cases, not all items were ranked as 3 unless there was a good indicator that the species relied primarily on those food sources. Medians and consensus (Tastle and Wierman 2007) of ranks were offered as a summary for each category. Consensus is a measure of statistical dispersion of ordinal data that measures the similarity of entries, with values ranging from 0 (no consensus; ranks are different among species) to 1 (full consensus; all ranks are equal among species).

Because of the recent description of *Canis lupaster* as distinct from *Canis aureus* (Koepfli et al. 2015), the diet of the former was based on information that originated from observations from Africa, and the diet of the latter from observations from Europe and Asia (Sillero-Zubiri et al. 2004). The diet of *Canis lycaon* was set to be equal to that of *C. lupus* because of their niche overlap, particularly when it comes to the consumption of large prey (Rutledge 2010). The diet for *Dusycyon australis* was mainly based on the prey available for that species on the Falkland Islands (Myers et al. 2018). A sensitivity analysis of downstream results showed that they are robust to perturbations in the ranking protocol (see the supplemental PDF for more information).

I tested the influence of diet on morphology using the phylogenetic multivariate linear model approach implemented in the package RRPP (Collyer and Adams 2018). This method has various desired properties (Adams 2014; Collyer et al. 2015). First, it allows one to account for the phylogenetic dependence among species in a generalized linear model context. Second, it is specifically designed for high-dimensional analyses, where the number of variables might exceed the number of observations. Third, because it produces a null distribution by a permutation procedure, it allows the analysis of nonnormal data, such as the diet data set. Morphological traits were standardized by the inverse of the square root of **P**. This standardization produces a space where Euclidean distances are equal to the Mahalanobis distance among observations in the original space (Mitteroecker and Bookstein 2011). Food items were considered as additive factors, using a type II sum of squares. The null distribution of effect sizes based on Cohen's *F* was built using 9,999 permutations.

### *Mapping Past Selection*

Directions and magnitudes of selection were quantified by calculating selection gradients ($\beta$) for each node of the Canidae phylogeny as follows:

$$\beta = \mathbf{G}^{-1}\Delta z, \tag{3}$$

where $\mathbf{G}^{-1}$ is the inverse of the genetic covariance and $\Delta z$ is the vector of morphometric changes (Lande 1979; Lofsvold 1988) calculated as PICs for each node (Felsenstein 1988). The selection gradient represents the directions of the morphospace for which the increase in fitness is the greatest and is a measure of selection independent of the patterns of covariation among traits. I applied the extension method to minimize the effect of sampling noise in the calculation of $\beta$'s (Marroig et al. 2012). This approach consists in artificially inflating the smallest eigenvalues in order to underplay their importance in the inverted matrix while still maintaining full rank. Following Marroig et al. (2012), the variance of the second derivative of eigenvalues was used to identify the noise floor region of $\mathbf{P}_w$. When the variance of the second derivative reached a floor level ($<$1E$-$8), all subsequent eigenvalues were substituted by the last reliable one (the one immediately before the noise floor region is reached). The extended matrix was used with equation (3) to obtain $\beta$'s relative to each node. $\beta$'s calculated in this way are the sum of selective pressures that happened during the divergence of the sister lineages referenced by each node (Turelli 1988) and are not to be taken as an expression of selection happening exclusively at the nodes.

I calculated the main selective lines of least resistance (SLLRs) to summarize the patterns of selection (Hohenlohe and Arnold 2008). SLLRs are the lines that have been most privileged by selection during evolution, or the eigenvectors of the effective adaptive landscape ($\boldsymbol{\Omega}$), which is defined as (Marroig and Cheverud 2010)

$$\Omega = \mathbf{G}^{-1}\mathbf{B}\mathbf{G}^{-1}. \tag{4}$$

Because **B** can be obtained as the average cross product of $\Delta z$ (Felsenstein 1988), the adaptive landscape can be obtained as

$$\Omega = \mathbf{G}^{-1}\Delta z \Delta z^{t}\mathbf{G}^{-1}\frac{1}{n}, \tag{5}$$

where $n$ is the number of contrasts. According to equations (3) and (5), it is easy to see that $\boldsymbol{\Omega}$ can be obtained

as the average cross product of the $\beta$'s. Gradients were scaled following Hansen and Houle's (2008) multivariate standardization to improve comparability among trait loadings. The leading eigenvectors of $\mathbf{\Omega}(\omega_i)$ were then interpreted as the main directions of selection (Marroig and Cheverud 2010). Because $\mathbf{\Omega}$ is estimated from a sample of $\beta$'s, it can suffer from the usual sampling bias for covariance matrices, namely, overestimation of the leading eigenvalues (Marroig et al. 2012). To evaluate whether the inferred pattern of selection could be retrieved in the absence of selection, I employed the same multivariate simulation procedure described previously for the eigenvalue regression. After each round of simulation, the produced $\Delta z$'s were scaled to have the same amount of variance as the empirical ones. The $n$ first empirical eigenvalues of $\mathbf{\Omega}$ that were proportionally larger than 95% of the simulated ones were then considered to be the main directions of selection ($\omega_i$, with $i = 1, \dots n$). Additionally, each $\omega_i$ was compared with $p_{\max}$ through vector correlation ($\vec{\rho}$) to evaluate whether selection was being applied along the main direction of phenotypic/genotypic variation.

The SLLRs ($\omega_i$) were further described in terms of dietary pressures by obtaining dietary-specific selection gradients ($\beta_{\text{diet}}$). These gradients were calculated by employing equation (3) and using the partial regression slopes produced by the RRPP regression analysis as idealized dietary $\Delta z$'s ($\Delta z_{\text{diet}}$). Each $\Delta z_{\text{diet}}$ indicates the direction in which the rate of change in morphological variables is most associated with the rate of change in the importance of a particular food item. These vectors were multiplied by the square root of $\mathbf{P}_{\text{w}}$ to restore them to the original log(cm) scale before calculating their corresponding selection gradients. The resulting $\beta_{\text{diet}}$ vectors were standardized and compared with $\omega_i$ through vector correlation ($\vec{\rho}$). Significance was assessed by confronting the observed value against the correlation obtained between $\omega_i$ and 1,000 random $\beta$'s drawn from a spherical $\mathbf{\Omega}$ matrix. The $\beta_{\text{diet}}$ vectors were also projected onto the significant $\omega_i$ to visualize the association between diet and the SLLRs.

### *Constraints and Structural Equation Modeling*

To evaluate the effect of constraints on a multivariate system, one must be able to properly disentangle aspects pertaining to the direction and magnitude of selection and evolution. The reason for this is that even in the presence of strong constraints (i.e., attraction exerted by $g_{\max}$), the rate of evolution of a multivariate system will not necessarily slow down. In fact, the rate of evolution will mostly be a function of the total amount of additive genetic variance in the direction of selection (i.e., evolvability) and the strength of selection (Hansen and Houle 2008). On the other hand, if constraints are at play, the misalignment of selection and evolutionary response might negatively affect the adjustment of the phenotype to functional demands, leading to maladaptation in spite of high rates of evolution.

Here, I quantified constraints ($c$) as the amount of attraction exerted by $g_{\max}$ on the evolutionary response. This was done by obtaining the vector correlation of the evolutionary response with $p_{\max}$ as a substitute for $g_{\max}$ ($\vec{\rho}(\Delta z, p_{\max})$; Renaud et al. 2006; Marroig et al. 2009). Evolvability ($e$) was calculated as the amount of variance in $\mathbf{P}_{\text{w}}$ in the direction of each node-specific $\beta$ (Hansen and Houle 2008). Rates of evolution were measured as the norm of the vectors of multivariate PIC for both morphology ($||\Delta z||$) and dietary data ($||\Delta d||$). The norm gives the size of a multivariate vector as the square root of the sum of its squares. In an unscaled contrast vector (or any difference between two points in the morphospace), the norm would give the amount of difference between the two points according to the Pythagorean theorem. Because the vectors here are time standardized, norms of these vectors are time standardized as well, producing a single estimate of multivariate evolutionary rates for a given node. Similarly, the strength of selection was measured as the norm of each selection gradient ($||\beta||$). Strength of selection was quantified only for the SLLRs considered significant according to the simulation approach described in the previous section. This was done by projecting each $\beta$ on the significant $\omega_i$ (back scaled to be on the same scale as the node-specific $\beta$) and calculating the norm in this reduced space. Last, to evaluate the influence of the main lines of selection $\omega_i$ on the adaptive evolution of the group, I calculated the vector correlation between each selection gradient and each SLLR ($\vec{\rho}(\beta, \omega_i)$). By calculating both strength and direction of selection only for the significant $\omega_i$, I ensure that both statistics are comparable. All statistics were calculated for each node of the phylogeny based on independent contrasts. By doing so, I ensure that any analysis of association among these statistics is considered within a phylogenetic comparative context.

Because of the complex theoretical connections between those variables, I employed the structural equation modeling (SEM) approach to explicitly model the relation among factors. As stated above, rates of morphological evolution are mostly a function of evolvability and strength of selection and were therefore modeled as such ($||\Delta z|| \sim e + ||\Delta\beta||$). Because the effect that $p_{\max}$ exerts on the evolutionary response can also be highly influenced by the direction of selection (Simon et al. 2016), constraints were modeled as a function of the alignment of the selection gradients with each SLLR ($c \sim \vec{\rho}(\beta, \omega_1) + \vec{\rho}(\beta, \omega_2) + \cdots + \vec{\rho}(\beta, \omega_n)$). To inspect the effect of constraints on ecology, I modeled the rates of dietary evolution

as a function of both the rates of morphological evolution (as would be expected if ecology and morphology coevolve) and constraints ($||\Delta d|| \sim ||\Delta z|| + c$). Thus, if constraints were at play, one would expect to see a negative coefficient of regression for the association between the deflection exerted by $p_{max}$ ($c$) and the rates of dietary evolution ($||\Delta d||$). Finally, I allowed all lower-level independent variables ($e$, $||\beta||$, and $\vec{\rho}(\beta, \omega_i)$)to covary with each other.

Ecology was modeled as a function of morphology because if constraints are at play, they will impede ecomorphological adaptation (morphology-ecology associations) without stopping all morphological change (Blows and Walsh 2009). Nevertheless, additional models that considered the relationship between $||\Delta d||$ and $||\Delta z||$ as a covariance instead of a regression were also tested and confronted with the simpler model above using the Akaike information criterion (AIC; Akaike 1974).

All variables were log transformed, with the exception of vector correlations, which were Fisher $z$ transformed to ensure normality. Variables were further centered and scaled to have 1 standard deviation. By doing this, all coefficients of the SEM are comparable to each other. The model was fit to the data using both maximum likelihood (Rosseel 2012) and Bayesian (Merkle and Rosseel 2018) approaches. The Bayesian version was run with default noninformative priors, three Markov chains, 500,000 interactions, 10% burn-in, and 10,000 samples.

## Results

### *Adaptive Evolution*

The PCA of the $\mathbf{P}_w$ matrix shows that the variation is highly concentrated on the first PC, $p_{max}$, which explains 31.63% of the total intraspecific variance. The second, third, and fourth PCs explain 10.07%, 7.18%, and 5.02%, respectively, of the variance, with all subsequent PCs explaining less than 5% of the variation. Vector correlation analysis shows that among all PCs, PC1 was the only one strongly associated with an isometric size vector ($\vec{\rho} = 0.965$), suggesting that $p_{max}$ for Canidae represents a size component.

The analysis of the variance of the second derivative of eigenvalues of $\mathbf{P}_w$ shows that the noise floor region is reached after the thirtieth eigenvector (fig. S1), suggesting that all further PCs are dominated by sampling noise. If this is the case, then any matrix inversion performed on $\mathbf{P}_w$ would lead to a matrix dominated by noise and would thus be unreliable for estimating past selection gradients. A simulation analysis was conducted to both confirm this interpretation and evaluate the usefulness of the extension approach in correcting for this issue. The results of this simulation show that nonextended matrices produce unreliable selection gradient estimates, while extended matrices significantly improve the procedure (see the supplemental PDF; fig. S2). Therefore, the extended version of $\mathbf{P}_w$ was used for all downstream analyses that required matrix inversion. Furthermore, I evaluated only the first 30 PCs in the eigenvalue regression analysis. Excluding the last 10 PCs led to a negligible loss of variance at both intraspecific (~1.05%) and interspecific (~0.13%) levels.

The inspection of the relationship between intraspecific variance ($\mathbf{P}_w$ eigenvalues, or $\lambda_P$) and rates of evolution (PC variance of $var_B$) shows a very strong positive association (fig. 2), with the leading PCs of $\mathbf{P}_w$ presenting higher rates of evolution than smaller PCs. Evolutionary simulations under drift produced a distribution of coefficients of proportionality $b$ with a mean and median of 0.999, a minimum of 0.861, and a maximum of 1.119. The empirical estimate of $b$ between $var_B$ and $\lambda_P$ was 1.244, falling outside the 95% interval for the null expectation ($Q_{0.025} = 0.924$, $Q_{0.975} = 1.075$; fig. 2). Most of the signal, however, was produced by the leading eigenvalue, which refers to $p_{max}$. The removal of the leading eigenvalue led to a decrease in the value of the coefficient of proportionality ($b = 1.001$), falling within the expectation under drift.

### *Dietary Data and Ecomorphology*

The literature review showed that canids have a widely varied diet. Median ranks for most dietary items were 2, with a few exceptions with lower ranks such as 1 and 0 (table 2). No single item had a median of 3, suggesting that canids do not heavily rely on any single food source. The consensus statistic was similar for all food items, ranging from 0.55 to 0.61, with the exception of large mammals, which had a consensus of 0.735. Overall, dietary ranks seem to be idiosyncratically dispersed along taxonomic groups, with the exception of large mammals, which shows low ranks for Vulpines and Cerdocyonina and higher ranks in a few taxa in Cerdocyonina (*Speothos venaticus* and *Dusycyon australis*) and in Canina, specifically in the genera *Cuon*, *Lycaon*, and *Canis*. Vertebrate food items had higher medians, with the exception of large mammals and fish, both of which had a median rank of 0. Among invertebrate items, hard-bodied prey had a higher median rank (2) than soft-bodied ones (median rank of 0). Among plant items, all median ranks were low (0), with the exception of fruit (median rank of 2).

The nonparametric RRPP regression showed that 10 out of 13 food items were significantly associated with morphology, explaining 39.81% of the total variation (table 3). The only food items not associated with morphology were small mammals, birds, and carrion. Among the

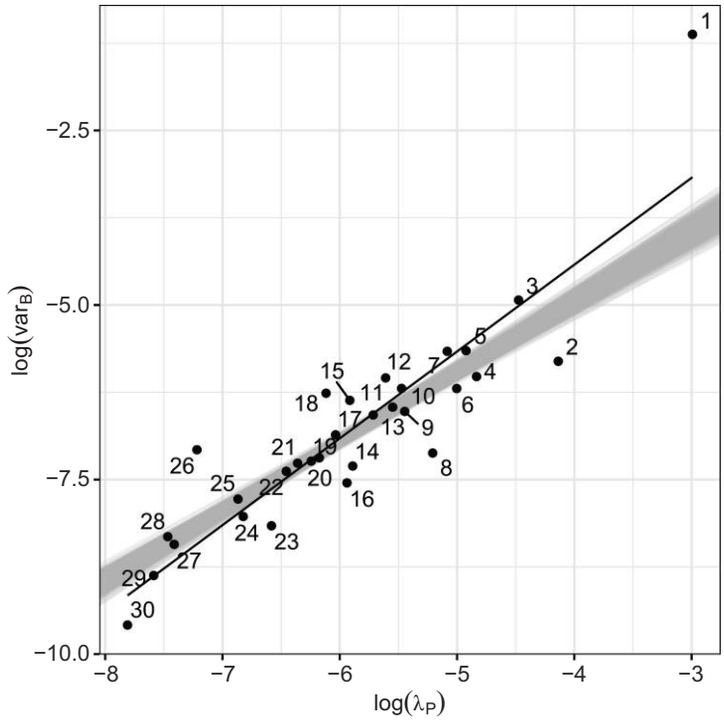


**Figure 2:** Eigenvalue regression test for proportionality between patterns of intra- and interspecific variation ($\mathbf{P}_w$ and $\mathbf{B}$, respectively). $\lambda_P$ = eigenvalues of $\mathbf{P}_w$; $\text{var}_B$ = variances of $\mathbf{B}$ projected onto the eigenvectors of $\mathbf{P}_w$, or the rate of evolution of the principal components of $\mathbf{P}_w$. Numbers refer to the retained principal components of $\mathbf{P}_w$. Black line = least squares linear regression. Gray lines = simulated regressions under no selection (genetic drift).

significant items, nonvertebrate food items (plants and invertebrates) had the largest effect sizes ($Z$-scores). Among vertebrate items, the consumption of large mammals had the largest effect size. Furthermore, the consumption of large mammals also explained the largest amount of variance among all dietary items ($R^2 = 0.059$). Diet-specific morphological changes ($\Delta z_{\text{diet}}$) and selection gradients ($\beta_{\text{diet}}$) can be found in the supplemental PDF (Machado 2020).

### *Mapping Past Selection*

Evolutionary simulations revealed that only the first two eigenvalues of the adaptive landscape $\mathbf{\Omega}$ were greater than expected by drift (fig. S3). Among all axes, $\omega_1$ was the only one strongly associated with $p_{\max}$ ($\vec{\rho}(\omega_1, p_{\max}) = 0.854$). The first axis ($\omega_1$) depicts a coordinated selection on all cranial traits that is generally in the same direction and of similar intensity (fig. 3; see table S3 for numeric values), with the exception of some optic and basicranial traits, which showed values close to zero. Taken together, both the direction of selection and association with $p_{\max}$ suggest that this axis basically corresponds to a selection for increase and decrease in overall size of the skull. Vector correlations between $\omega_1$ and $\beta_{\text{diet}}$ show that this axis is mainly associated with changes in the importance of nonvertebrate dietary items (table 3; fig. 3). Specifically, this analysis suggests that selection for size increase is positively associated with selection for increased consumption of fruit, roots, eggs, and soft-bodied invertebrates and negatively associated with selection for consumption of seeds, leaves, hard-bodied invertebrates, and herptiles. Selection for consumption of large and small mammals was moderately associated with this axis with opposite signs (positive association with the former and negative association with the latter; fig. 3).

The second axis ($\omega_2$) depicts strong negative selection on characters representing overall facial length and positive selection for increased facial and skull height (fig. 3). Selection on optic traits was ambiguous: while anteroposterior dimensions were negatively associated with $\omega_2$, dorsoventral dimensions and the distance between the posterior portion of the orbit and the neurocranium were positively associated with this axis. Last, traits associated with mastication, like teeth size and the size of the zygomatic arch, were positively associated with $\omega_2$. Vector correlations show that this direction of selection is mostly associated with the importance of vertebrate taxa in the diet.

**Table 2:** Importance of food items in diet of canid species

| Group and species | Large mammals | Small mammals | Birds | Herptiles | Fish | Eggs | Carrion | Hard-bodied invertebrates | Small-bodied invertebrates | Seeds | Fruits | Roots | Leaves |
|---|---|---|---|---|---|---|---|---|---|---|---|---|---|
| Vulpines: | | | | | | | | | | | | | |
| *U. littoralis* | 0 | 2 | 2 | 1 | 0 | 2 | 1 | 3 | 1 | 0 | 3 | 0 | 1 |
| *U. cinereoargenteus* | 0 | 3 | 2 | 0 | 0 | 1 | 1 | 2 | 0 | 1 | 3 | 1 | 0 |
| *N. procyonoides* | 0 | 2 | 2 | 2 | 2 | 2 | 2 | 2 | 2 | 2 | 2 | 2 | 2 |
| *O. megalotis* | 0 | 1 | 1 | 1 | 0 | 1 | 0 | 3 | 0 | 0 | 0 | 0 | 0 |
| *V. pallida* | 0 | 2 | 2 | 2 | 0 | 2 | 0 | 2 | 0 | 0 | 2 | 0 | 0 |
| *V. chama* | 0 | 3 | 0 | 2 | 0 | 0 | 2 | 2 | 2 | 0 | 0 | 0 | 0 |
| *V. bengalensis* | 0 | 2 | 2 | 2 | 0 | 2 | 0 | 2 | 0 | 0 | 2 | 0 | 0 |
| *V. zerda* | 0 | 2 | 2 | 2 | 0 | 2 | 2 | 3 | 0 | 0 | 2 | 2 | 2 |
| *V. lagopus* | 0 | 3 | 2 | 0 | 2 | 2 | 2 | 2 | 2 | 0 | 0 | 0 | 0 |
| *V. velox* | 0 | 2 | 2 | 2 | 2 | 2 | 2 | 2 | 0 | 2 | 2 | 0 | 0 |
| *V. macrotis* | 0 | 3 | 2 | 2 | 0 | 0 | 2 | 2 | 0 | 0 | 2 | 0 | 0 |
| *V. vulpes* | 1 | 3 | 2 | 2 | 2 | 2 | 2 | 2 | 1 | 0 | 3 | 2 | 2 |
| *V. rueppellii* | 0 | 2 | 2 | 2 | 0 | 2 | 0 | 3 | 0 | 0 | 0 | 2 | 2 |
| *V. corsac* | 0 | 3 | 2 | 0 | 0 | 0 | 2 | 2 | 0 | 0 | 2 | 0 | 0 |
| *V. ferrilata* | 0 | 3 | 3 | 0 | 0 | 1 | 0 | 1 | 1 | 0 | 0 | 0 | 0 |
| Cerdocyonina: | | | | | | | | | | | | | |
| *A. microtis* | 0 | 3 | 1 | 1 | 3 | 0 | 0 | 2 | 0 | 0 | 2 | 0 | 1 |
| *C. thous* | 0 | 3 | 3 | 2 | 1 | 2 | 2 | 2 | 0 | 0 | 2 | 0 | 0 |
| *L. fulvipes* | 0 | 2 | 2 | 2 | 0 | 0 | 2 | 2 | 0 | 2 | 2 | 0 | 0 |
| *L. sechurae* | 0 | 2 | 2 | 1 | 0 | 2 | 2 | 2 | 0 | 3 | 3 | 0 | 0 |
| *L. gymnocercus* | 1 | 3 | 2 | 2 | 1 | 1 | 2 | 2 | 1 | 0 | 1 | 0 | 0 |

| | | | | | | | | | | | | | |
|---|---|---|---|---|---|---|---|---|---|---|---|---|---|
| *L. griseus* | 0 | 3 | 2 | 2 | 0 | 2 | 3 | 2 | 0 | 2 | 2 | 0 | 0 |
| *L. vetulus* | 0 | 2 | 2 | 2 | 0 | 0 | 0 | 3 | 0 | 0 | 2 | 0 | 0 |
| *L. culpaeus* | 2 | 3 | 2 | 2 | 0 | 0 | 2 | 2 | 2 | 0 | 2 | 0 | 0 |
| *S. venaticus* | 3 | 2 | 1 | 1 | 1 | 0 | 0 | 1 | 1 | 0 | 1 | 0 | 0 |
| *D. australis* | 2 | 0 | 3 | 3 | 2 | 0 | 3 | 2 | 2 | 0 | 0 | 0 | 0 |
| *C. brachyurus* | 0 | 3 | 2 | 2 | 1 | 2 | 0 | 2 | 2 | 0 | 3 | 2 | 0 |
| Canina: | | | | | | | | | | | | | |
| *L. mesomelas* | 2 | 3 | 2 | 1 | 2 | 0 | 1 | 3 | 1 | 0 | 1 | 0 | 0 |
| *L. adusta* | 1 | 2 | 2 | 2 | 0 | 0 | 3 | 3 | 0 | 0 | 2 | 0 | 0 |
| *C. alpinus* | 3 | 2 | 2 | 1 | 0 | 0 | 1 | 1 | 0 | 0 | 1 | 0 | 0 |
| *L. pictus* | 3 | 2 | 1 | 1 | 0 | 1 | 1 | 0 | 0 | 0 | 0 | 0 | 1 |
| *C. aureus* | 2 | 3 | 3 | 2 | 2 | 2 | 0 | 2 | 2 | 2 | 2 | 2 | 2 |
| *C. simensis* | 1 | 3 | 2 | 0 | 0 | 2 | 1 | 0 | 0 | 0 | 0 | 0 | 1 |
| *C. latrans* | 2 | 3 | 1 | 1 | 1 | 0 | 2 | 1 | 1 | 1 | 2 | 1 | 1 |
| *C. lupaster* | 1 | 3 | 2 | 2 | 0 | 0 | 2 | 2 | 2 | 0 | 1 | 0 | 0 |
| *C. indica* | 3 | 2 | 2 | 2 | 2 | 0 | 2 | 0 | 0 | 0 | 0 | 0 | 0 |
| *C. himalayensis* | 3 | 2 | 2 | 1 | 1 | 0 | 1 | 0 | 0 | 0 | 0 | 0 | 0 |
| *C. lupus* | 3 | 2 | 2 | 1 | 1 | 1 | 1 | 1 | 0 | 0 | 1 | 0 | 0 |
| *C. lycaon* | 3 | 2 | 2 | 1 | 1 | 1 | 1 | 1 | 0 | 0 | 1 | 0 | 0 |
| *C. rufus* | 2 | 3 | 1 | 0 | 0 | 0 | 2 | 1 | 0 | 0 | 1 | 0 | 0 |
| Median | 0 | 2 | 2 | 2 | 0 | 1 | 2 | 2 | 0 | 0 | 2 | 0 | 0 |
| Consensus | .735 | .554 | .561 | .582 | .559 | .574 | .564 | .589 | .586 | .599 | .579 | .610 | .534 |

Note: Ranks refer to the relative importance of food items, ranging from 0 (not consumed) to 3 (primary food sources). See text for more details on the ranking scheme.

**Table 3:** Relationship between diet, selection, and morphology

| | Linear model | | | | | | Vector correlations | |
|---|---|---|---|---|---|---|---|---|
| Diet | df | SS | $R^2$ | $F$ | $Z$ | $P$ | $\omega_1$ | $\omega_2$ |
| Large mammals | 1 | 52.296 | .059 | 3.153 | 3.106 | **.001** | **.529** | **.630** |
| Small mammals | 1 | 19.250 | .022 | 1.160 | 1.382 | .090 | **−.444** | −.211 |
| Birds | 1 | 20.640 | .023 | 1.244 | 1.558 | .069 | .177 | **−.634** |
| Herptiles | 1 | 25.677 | .029 | 1.548 | 1.901 | **.039** | **−.817** | −.190 |
| Fish | 1 | 30.178 | .034 | 1.819 | 2.338 | **.013** | .165 | **.538** |
| Eggs | 1 | 36.056 | .041 | 2.174 | 2.641 | **.007** | **.818** | .098 |
| Carrion | 1 | 19.440 | .022 | 1.172 | 1.609 | .064 | .180 | **−.523** |
| Hard-bodied invertebrates | 1 | 34.724 | .039 | 2.093 | 2.647 | **.006** | **−.706** | .187 |
| Soft-bodied invertebrates | 1 | 35.396 | .040 | 2.134 | 2.734 | **.005** | **.823** | −.153 |
| Seeds | 1 | 39.303 | .045 | 2.369 | 2.979 | **.003** | **−.725** | .152 |
| Leaves | 1 | 49.171 | .056 | 2.964 | 3.492 | **.001** | **−.844** | −.009 |
| Roots | 1 | 27.722 | .032 | 1.671 | 2.651 | **.008** | **.659** | −.233 |
| Fruit | 1 | 19.528 | .022 | 1.177 | 2.068 | **.027** | **.735** | .098 |
| Residuals | 25 | 414.701 | .472 | | | | | |
| Total | 38 | 879.222 | | | | | | |

Note: Linear model shows results of the nonparametric RRPP multiple regression of the relationship between morphology and diet. SS = type II sum of squares; $R^2$ = coefficient of determination. $F$ = pseudo $F$-statistic; $Z$ = standardized $Z$-scores based on Cohen's $F$; $P$ = probability of the observed $Z$-score given the null hypothesis of no association. Values in bold are significant ($\alpha < 0.05$). Null distribution built with 9,999 permutations. Vector correlations are between diet-specific selection gradients ($\beta_{diet}$) and the first two eigenvectors of the adaptive landscape $\boldsymbol{\Omega}$.

Specifically, $\omega_2$ is positively associated with selection for the consumption of large mammals—as well as fish to a lesser degree—and negatively associated with selection for other terrestrial vertebrate items, particularly birds and carrion (table 3; fig. 3). Because these two vectors were the only ones considered significant in the evolutionary simulation approach, they are the only ones used for the computation of direction and magnitude of selection in the SEM analyses.

### *Constraints and Structural Equation Modeling*

Among the SEM models tested, the one modeling the relationship between ecological rates and morphological rates as a regression had the lowest AIC in the maximum likelihood analysis ($AIC_{covariance} = 679.081$, $AIC_{regression} = 675.431$). An inspection of the coefficients shows that general interpretations drawn from both models are similar (table S5), so here I discuss only the regression model.

Coefficients of regression and covariances estimated for the SEM model were similar between maximum likelihood and Bayesian analyses (table S6), and therefore I focus on the latter for simplicity (fig. 4). The covariance estimates suggest that there is a positive connection between evolvability ($e$) and the alignment of selection with the first SLLR ($\vec{\rho}(\beta, \omega_1)$). The same was not true for the alignment of selection with the second SLLR ($\vec{\rho}(\beta, \omega_2)$), which seems to be positively associated with strength of selection ($||\beta||$) instead. A negative association between $\vec{\rho}(\beta, \omega_1)$ and $\vec{\rho}(\beta, \omega_2)$ was also detected, suggesting that selection gradients cannot be strongly aligned with both SLLRs at the same time.

The regression coefficients show that both strength of selection and evolvability are good predictors of the rate of morphological evolution ($||\Delta z||$), as expected, with a large portion of the variance of $||\Delta z||$ being explained by those two factors ($R^2 = 0.687$). On the other hand, alignments with the first SLLRs could only partially explain the attracting influence of $p_{max}$ (i.e., constraints, $c$). While $\vec{\rho}(\beta, \omega_1)$ showed a positive influence on $c$, only a small portion of the variance in $c$ could be explained by this factor ($R^2 = 0.192$). Despite this, both $c$ and $||\Delta z||$ were associated with the rate of dietary evolution ($||\Delta d||$), explaining a moderate amount of the variance of $||\Delta d||$ ($R^2 = 0.462$). As expected, these factors had different associations with $||\Delta d||$: while $||\Delta z||$ was positively and strongly associated with $||\Delta d||$, the contribution of $c$ was moderate and negative. In other words, the rate of morphological change was more important in determining the rate of dietary evolution, but the presence of a negative association between the direction of morphological evolution and the evolution of diet suggests the action of constraints on the system.

## Discussion

The role of the association among parts in shaping macroevolutionary patterns has always been a topic of intense debate (Gould and Lewontin 1979; Maynard Smith et al. 1985; Jablonski 2019). While covariances between

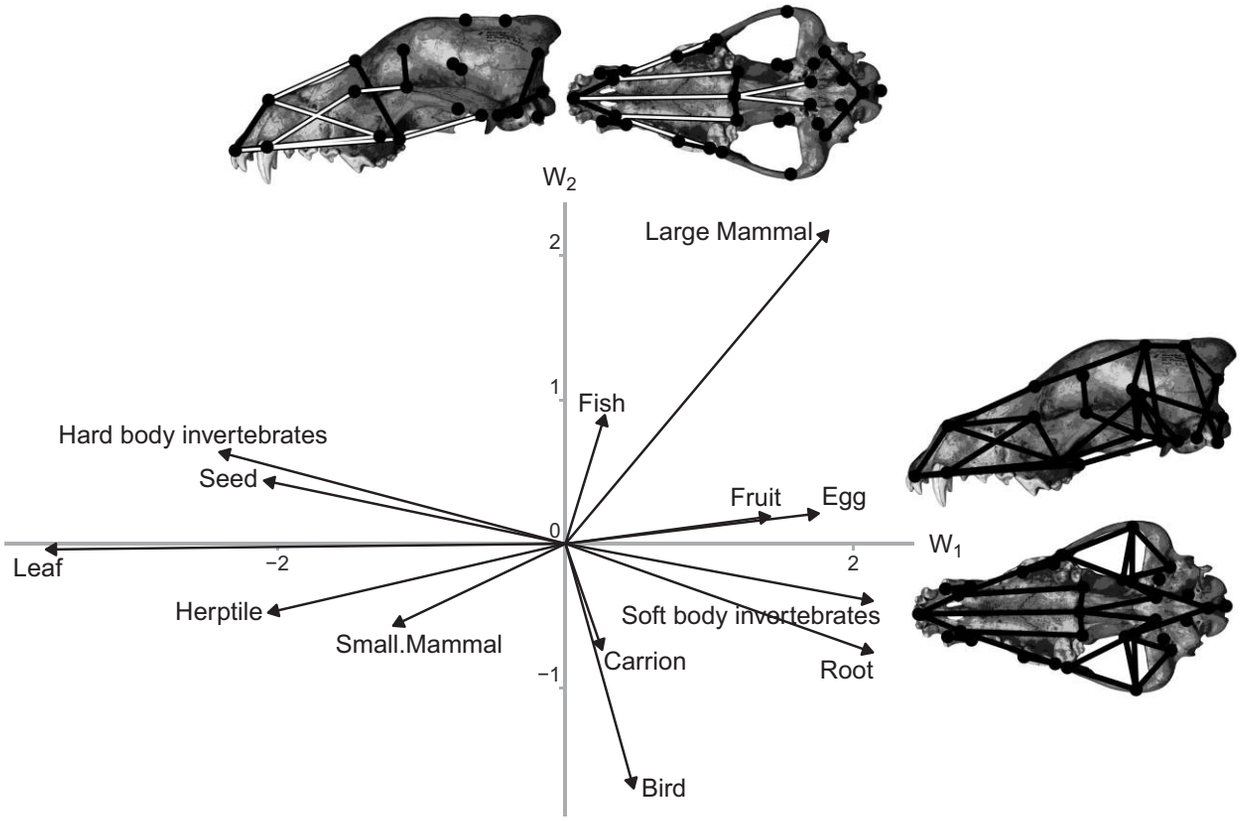


**Figure 3:** First two eigenvectors of the adaptive landscape matrix **Ω**. *Canis lupus* skulls display the normalized coefficient of selection on each of the interlandmark traits associated with positive selection along each axis. Positive values are depicted with black lines and negative values with white lines. Arrows represent the projections of diet-specific selection gradients onto the first two eigenvectors.

traits are expected to constrain immediate evolutionary responses (Lande 1979), these effects are usually thought to be erased over longer timescales (Schluter 1996; Arnold et al. 2001). The results shown here contradict this hypothesis, showing that rates of evolution in Canidae were similar to patterns of intraspecific phenotypic variance (fig. 2), which suggests the influence of constraints on a macroevolutionary scale. Additionally, patterns of morphological evolution were shown to not conform to what was expected under drift (fig. 2) and are partially explained by differences in diet (table 3). Inspection of the SLLR of the adaptive landscape indicated that selection acted on both size and shape (nonsize) components (fig. 3). While most hypothetical dietary selective gradients align themselves with size, selection for the consumption of large mammals was associated with selection for both size and shape features of the skull (fig. 3; table 3). Last, SEM showed that alignment of selection with size had a constraining effect on morphological evolution, which in turn hindered ecological adaptation in the group (fig. 4). Together, these results show that not only can genetic and developmental constraints affect evolutionary patterns on larger timescales but also they can slow down ecological adaptation.

The proposition that ontogenetic constrains interfere with macroevolutionary patterns is not exclusive to canids. Specifically, recent work has recurrently shown that macroevolutionary rates of evolution (**B** here) tend to mimic intraspecific patterns of variation ($\mathbf{P}_w$ here) in a wide variety of taxa, ranging from *Drosophila* (Houle et al. 2017) to amphibians (Simon et al. 2016), lizards (McGlothlin et al. 2018), and mammals (e.g., Marroig and Cheverud 2004; Firmat et al. 2014; De Azevedo et al. 2017). Works on highly multivariate systems show that the leading eigenvector of within-group covariance ($p_{max}$ or size here) tends to be an effective source of constraints for evolution (Marroig and Cheverud 2010; Simon et al. 2016). This is further evidenced here by the fact that $p_{max}$ showed rates of evolution that were proportionally higher than those expected under drift (proportionality between **B** and $\mathbf{P}_w$; fig. 2).

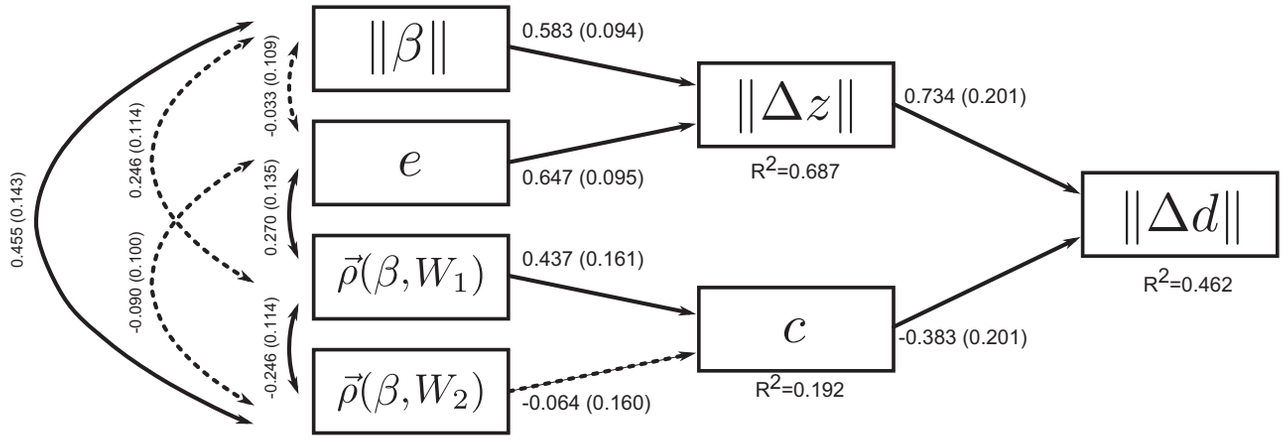


**Figure 4:** Path-like diagram representing the structural equation modeling. $\vee\beta\vee$ = strength or magnitude of selection; $e$ = evolvability; $\vec{\rho}(\beta, \omega_1)$ = alignment of selection with the first selective line of least resistance (SLLR); $\vec{\rho}(\beta, \omega_2)$ = alignment of selection with the second SLLR; $\vee\Delta z\vee$ = rate of morphological evolution; $c$ = alignment of morphological change with $p_{max}$ (i.e., constraints); $\vee\Delta d\vee$ = rate of dietary evolution. Straight arrows = direct dependence between variables, with the independent variable at the origin and the dependent at the end. Curved arrows = covariance between traits. Dashed lines represent the nonsignificant coefficients on the maximum likelihood analysis. Values along the lines (curved lines) or at their origin (straight lines) are the path coefficients (slope coefficients or covariances, respectively) for the Bayesian analysis. All path coefficients are accompanied by their respective standard deviation of the posterior distribution in parentheses. Values below boxes are the coefficient of determination $R^2$. See table S5 (available online) for the full list of coefficients and $R^2$ values for both maximum likelihood and Bayesian analyses.

The channeling of morphological evolution along $p_{max}$, however, does not allow one to discern between evolution aligned with $p_{max}$ as a product of direct selection on size or as a by-product of indirect selection on shape (nonsize) variables plus the action of intraspecific multivariate constraints (Marroig and Cheverud 2010). In the first scenario, evolutionary responses would not be deflected away from $\beta$ given that selection is already aligned with $p_{max}/g_{max}$. Furthermore, because these lines are the directions in which evolvability is highest, rates of evolutionary responses would be potentialized (Hansen and Houle 2008). In the second scenario, selection is not aligned with $p_{max}/g_{max}$, and constraints force the evolutionary response to align with $p_{max}/g_{max}$ (Schluter 1996). The reconstruction of past selective regimes suggests that both factors might have acted in shaping morphological diversity in Canidae. While the main SLLR $\omega_1$ is indeed aligned with size, the evolutionary modeling approach was also able to recover a secondary SLLR, $\omega_2$, associated exclusively with shape changes (fig. 3). Morphological features associated with $\omega_2$ are readily interpretable in terms of performance and ecological demands. For example, the shortening of facial length reduces strain in the skull due to biting struggling prey or crushing bones (Werdelin 1989; Covey and Greaves 1994; Slater et al. 2009), while larger zygomatic arches would support greater bite forces (Ellis et al. 2009; Damasceno et al. 2013; Penrose et al. 2016). Increase in tooth size supplements these demands, as enlarged canines would increase the efficiency of kill-bites (Van Valkenburgh and Koepfli 1993; Therrien 2005), and larger carnassial teeth could improve the performance in processing meat and bones (Greaves 1983; Van Valkenburgh 1988; Werdelin 1989; Biknevicius and Ruff 1992; Therrien 2005). An increase in the height of the rostrum could compensate for the loss of turbinate area due to reduction of the rostrum, maintaining or even increasing olfactory capacity (Green et al. 2012). Finally, more forward-facing, convergent orbits would enhance stereoscopic vision and depth perception (Heesy 2008).

Because selection for functionally related traits seems to be a major aspect of the morphological evolution in Canidae, one would expect morphology and ecology to be tightly associated within the group. Here I have found that nearly 40% of the total variance in cranial morphology is associated with size, as expected (table 3). However, an inspection of the hypothetical dietary selection gradients ($\beta_{diet}$) shows that the majority of $\beta_{diet}$ vectors are more aligned with size ($\omega_1$) than with shape ($\omega_2$; table 3; fig. 3). Additionally, most of the items with highest effect sizes (invertebrates and plants) are more aligned with size, suggesting that their large influence on morphology is probably due to changes in size (table 3). Furthermore, the SEM analysis shows that the alignment of selection with $\omega_1$ is positively related to the attraction imposed by $p_{max}/g_{max}$ (or constraint), which in turn has a negative effect on rates of ecological evolution (fig. 4). In other words, even though selection for size is associated with selection for consumption of various food items, changes

produced as a consequence of selection will mostly result in size variation and not necessarily ecological changes. This is consistent with the idea that Canidae are considered to be functionally conserved among the Carnivora families (Werdelin and Wesley-Hunt 2014; Michaud et al. 2018).

Despite the constraining effect of trait covariation on the ecomorphological evolution of canids, some species exhibit morphological adaptations for hypercarnivory that largely agree with the ones described for $\omega_2$ here (Van Valkenburgh and Koepfli 1993; Slater et al. 2009; Green et al. 2012; Damasceno et al. 2013). This suggests that selection for the consumption of large mammalian prey is being translated into morphological changes despite the presence of constraints, as suggested by the fact that large mammals were the main dietary item influencing the skull form (table 3). Curiously enough, selection for large mammal consumption was the only dietary item that was significantly aligned with both SLLRs (table 3). Additionally, $\beta_{\text{diet}}$ for large mammals was the largest (fig. 3), suggesting that the strength of selection was greatest along this direction. While the alignment with $\omega_1$ might have acted negatively on the ecological evolution along these lines, an increased strength of selection might have caused increased rates of morphological evolution, leading to ecological adaptation (fig. 4).

It is worth noticing that the directions of selection estimated here, both SLLR and $\beta_{\text{diet}}$, are estimated for the whole clade, a fact that might mask selective pressures that happened at a smaller scale. In the case of the consumption of large mammals, this might mean that the selection in the directions of size ($\omega_1$) and shape ($\omega_2$) have acted in different moments: it is possible that initial selection for consuming large mammals was less intense in the direction of $\omega_2$, ensuring that both direct selection for size and constraints on shape selection would produce size increases. However, as canids increase in size, they usually get disproportionately larger faces (Wayne 1986; Penrose et al. 2016; Machado et al. 2018; Machado and Teta 2020), a fact that would result in poorer biomechanical performance and bite forces (Radinsky 1981; Van Valkenburgh and Koepfli 1993; Ellis et al. 2009; Slater et al. 2009; Damasceno et al. 2013). This conflict might not be relevant until species reach a certain size threshold, where energetic demands and foraging cost scale greatly, requiring a switch to a specialized hypercarnivorous diet in order to balance the energetic budget (Vézina 1985; Carbone et al. 1999, 2007; Clauss et al. 2010; Tucker et al. 2016; De Cuyper et al. 2018). Because increasing in size might be too energetically costly at that point, large predators might be under more intense selection to change shape ($\omega_2$), not size ($\omega_1$), in order to improve performance (Segura et al. 2020). Given that selection for shape is not aligned with $g_{\text{max}}$, stronger selection might be necessary to overcome constraints (figs. 3, 4), putting large predators on a higher populational strain than nonspecialists or smaller species (Villmoare 2013). In conjunction with the fact that larger carnivores tend to present smaller population sizes, this would make large specialist canids susceptible to population decline and ultimately to higher rates of extinction (Van Valkenburgh et al. 2004). Alternatively, ecomorphological specialization might lead to a reduction of the morphospace occupied by hypercarnivores, ultimately reducing the capacity of a clade to adapt to different environmental pressures (Holliday and Steppan 2004). Together, these processes could help explain why hypercarnivory specifically—or a specialized ecology in general—is detrimental to species longevity in the fossil record (Balisi et al. 2018).

The conclusion that Canidae morphological evolution was affected by multivariate constraints may seem at odds with previous evidence showing that the group in fact has an increased evolutionary potential in the facial region (Machado et al. 2018, 2019). This apparent conflict might be explained by at least four hypothesis. First, the increased evolutionary potential of Canidae seems to be associated with increases in the allometric relation between size and facial traits (Machado et al. 2018). This means that the increased flexibility observed for Canidae is correlated with size through allometry, suggesting that selection for localized shape changes in the facial region could still produce associated size changes through the action of constraints. Second, it could be the case that ecological opportunities do not align with those increased evolutionary potentials, producing evolutionary responses that are still highly constrained (Segura et al. 2020). Third, because canid morphology is well suited to a variety of ecological roles, strong selection on shape variables may be necessary in only extreme cases, such as in hypercarnivore taxa, making it harder to identify the signal of selection for shape features. In other words, broadscale comparisons such as the one presented here might fail to evaluate morphological evolution that is happening at a more restricted taxonomic level (Van Valkenburgh and Wayne 1994; Machado and Teta 2020). Fourth, extant species of canids occupy only a small portion of the morphospace for the family, thereby hiding much of the ecomorphological signal that can be retrieved (Wang 1994; Wang et al. 1999; Tedford et al. 2009). Because the fossil record of the group is rich with diverse kinds of predatory forms (Van Valkenburgh 2007; Slater 2015), it might be the case that a more thorough inspection of extinct species will reveal a more complex selective regime. More investigations on the fossil record of the group along with comparisons with different taxa might help us to understand the relative importance of each of these factors in shaping morphological evolution in the presence of multivariate constraints.

## Acknowledgments

I am deeply indebted to Pablo Teta for all the support he provided during my postdoc fellowship at the Museo de Historia Natural "Bernardino Rivadavia." I thank Thiago M. G. Zahn and Alex Hubbe for their diligent proofreading and commenting and Scott J. Steppan, Graham Slater, and three anonymous reviewers for their insightful remarks. I also thank the curatorial staff who provided help and access to zoological collections: Mário de Vivo and Juliana Gualda (Museu de Zoologia da Universidade de São Paulo); João Oliveira, Luiz Flamarion, and Sérgio Maia Vaz (Museu Nacional, Universidade Federal do Rio de Janeiro); David Flores and Sergio Lucero (Museo Argentino de Ciencias Naturales "Bernardino Rivadavia"); Diego Verzi and Itati Olivares (Museo de La Plata); Eileen Lacey and Chris Conroy (Museum of Vertebrate Zoology); Nancy B. Simmons, Neil Duncan, Eileen Westwig, Aja Marcato, and Eleanor Hoeger (American Museum of Natural History); Kris Helgen, Darrin Lunde, Esther Langan, and John Ososky (Smithsonian National Museum of Natural History); Bruce Patterson and Bill Stanley (Field Museum); Hopi Hoekstra and Judith Chupasko (Museum of Comparative Zoology); and Ted Daeschler and Ned Gilmore (Academy of Natural Sciences of Drexel University). This research was partially supported by grants from the Fundação de Amparo à Pesquisa do Estado de São Paulo (FAPESP; 2011/21674-4, 2013/22042-7) and the National Science Foundation (DEB 1350474 to L. Revell).

## Literature Cited

Ackermann, R. R., and J. M. Cheverud. 2002. Discerning evolutionary processes in patterns of tamarin (genus *Saguinus*) craniofacial variation. American Journal of Physical Anthropology 117:260–271.

Adams, D. C. 2014. A method for assessing phylogenetic least squares models for shape and other high-dimensional multivariate data. Evolution 68:2675–2688.

Akaike, H. 1974. A new look at the statistical model identification. IEEE Transactions on Automatic Control 19:716–723.

Arnold, S. J. 1992. Constraints on phenotypic evolution. American Naturalist 140(suppl.):S85–S107.

Arnold, S. J., M. Pfrender, and A. G. Jones. 2001. The adaptive landscape as a conceptual bridge between micro- and macroevolution. Genetica 112:9–32.

Arnold, S. J., and P. Phillips. 1999. Hierarchical comparison of genetic variance-covariance matrices. II. Coastal-inland divergence in the garter snake, *Thamnophis elegans*. Evolution 53:1516–1527.

Balisi, M., C. Casey, and B. Van Valkenburgh. 2018. Dietary specialization is linked to reduced species durations in North American fossil canids. Royal Society Open Science 5:171861.

Bekoff, M. 1977. *Canis latrans*. Mammalian Species 79:1–9.

Biknevicius, A. R., and C. B. Ruff. 1992. The structure of the mandibular corpus and its relationship to feeding behaviours in extant carnivorans. Journal of Zoology 228:479–507.

Blows, M., and B. Walsh. 2009. Spherical cows grazing in flatland: constraints to selection and adaptation. Pages 83–101 *in* J. van der Werf, H. U. Graser, R. Frankham, and C. Gondro, eds. Adaptation and fitness in animal populations. Vol. 39. Springer, Dordrecht.

Carbone, C., G. M. Mace, S. C. Roberts, and D. W. Macdonald. 1999. Energetic constraints on the diet of terrestrial carnivores. Nature 402:286–288.

Carbone, C., A. Teacher, and J. Rowcliffe. 2007. The costs of carnivory. PLoS Biology 5:363–368.

Cheverud, J. M. 1984. Quantitative genetics and developmental constraints on evolution by selection. Journal of Theoretical Biology 110:155–171.

———. 1988. A comparison of genetic and phenotypic correlations. Evolution 42:958–968.

Clark, H. O., Jr. 2005. *Otocyon megalotis*. Mammalian Species 766:1–5.

Clark, H. O., Jr, D. P. Newman, J. D. Murdoch, J. Tseng, Z. H. Wang, and R. B. Harris. 2008. *Vulpes ferrilata* (Carnivora: Canidae). Mammalian Species 821:1–6.

Clauss, M., H. Kleffner, and E. Kienzle. 2010. Carnivorous mammals: nutrient digestibility and energy evaluation. Zoo Biology 29:687–704.

Collyer, M. L., and D. C. Adams. 2018. RRPP: an R package for fitting linear models to high-dimensional data using residual randomization. Methods in Ecology and Evolution 9:1–23.

Collyer, M. L., D. J. Sekora, and D. C. Adams. 2015. A method for analysis of phenotypic change for phenotypes described by high-dimensional data. Heredity 115:357–365.

Cossíos, E. D. 2010. *Lycalopex sechurae* (Carnivora: Canidae). Mammalian Species 42:1–6.

Covey, D., and W. S. Greaves. 1994. Jaw dimensions and torsion resistance during canine biting in the Carnivora. Canadian Journal of Zoology 72:1055–1060.

Dalponte, J. C. 2009. *Lycalopex vetulus* (Carnivora: Canidae). Mammalian Species 847:1–7.

Damasceno, E. M., E. Hingst-Zaher, and D. Astúa. 2013. Bite force and encephalization in the Canidae (Mammalia: Carnivora). Journal of Zoology 290:246–254.

De Azevedo, S., M. F. González, C. Cintas, V. Ramallo, M. Quinto-Sánchez, F. Márquez, T. Hunemeier, et al. 2017. Nasal airflow simulations suggest convergent adaptation in Neanderthals and modern humans. Proceedings of the National Academy of Sciences of the USA 114:12442–12447.

De Cuyper, A., M. Clauss, C. Carbone, D. Codron, A. Cools, M. Hesta, and G. P. J. Janssens. 2018. Predator size and prey size-gut capacity ratios determine kill frequency and carcass production in terrestrial carnivorous mammals. Oikos 128:13–22.

Dietz, J. M. 1985. *Chrysocyon brachyurus*. Mammalian Species 234:1–4.

Ellis, J. L., J. Thomason, E. Kebreab, K. Zubair, and J. France. 2009. Cranial dimensions and forces of biting in the domestic dog. Journal of Anatomy 214:362–373.

Esteve-Altava, B., J. Marugán-Lobón, H. Botella, and D. Rasskin-Gutman. 2012. Structural constraints in the evolution of the tetrapod skull complexity: Williston's law revisited using network models. Evolutionary Biology 40:209–219.

Felsenstein, J. 1988. Phylogenies and quantitative characters. Annual Review of Ecology and Systematics 19:445–471.

Finarelli, J. A. 2010. Does encephalization correlate with life history or metabolic rate in Carnivora? Biology Letters 6:350–353.

Finarelli, J. A., and J. J. Flynn. 2009. Brain-size evolution and sociality in Carnivora. Proceedings of the National Academy of Sciences of the USA 106:9345–9349.

Finarelli, J. A., and A. Goswami. 2009. The evolution of orbit orientation and encephalization in the Carnivora (Mammalia). Journal of Anatomy 214:671–678.

Firmat, C., I. Lozano-Fernandez, J. Agusti, G. H. Bolstad, G. Cuenca-Bescos, T. F. Hansen, and C. Pélabon. 2014. Walk the line: 600000 years of molar evolution constrained by allometry in the fossil rodent *Mimomys savini*. Philosophical Transactions of the Royal Society B 369:20140057.

Gould, S. J., and Lewontin. 1979. The spandrels of San Marco and the Panglossian paradigm: a critique of the adaptationist programme. Proceedings of the Royal Society B 205:581–598.

Greaves, W. S. 1983. A functional analysis of carnassial biting. Biological Journal of the Linnean Society 20:353–363.

Green, P. A., B. Van Valkenburgh, B. Pang, D. Bird, T. Rowe, and A. Curtis. 2012. Respiratory and olfactory turbinal size in canid and arctoid carnivorans. Journal of Anatomy 221:609–621.

Hallgrímsson, B., H. Jamniczky, N. Young, C. Rolian, T. Parsons, J. Boughner, and R. S. Marcucio. 2009. Deciphering the palimpsest: studying the relationship between morphological integration and phenotypic covariation. Evolutionary Biology 36:355–376.

Hansen, T., and D. Houle. 2008. Measuring and comparing evolvability and constraint in multivariate characters. Journal of Evolutionary Biology 21:1201–1219.

Heesy, C. P. 2008. Ecomorphology of orbit orientation and the adaptive significance of binocular vision in primates and other mammals. Brain, Behavior, and Evolution 71:54–67.

Hohenlohe, P. A., and S. J. Arnold. 2008. MIPoD: a hypothesis-testing framework for microevolutionary inference from patterns of divergence. American Naturalist 171:366–385.

Holliday, J. A., and S. J. Steppan. 2004. Evolution of hypercarnivory: the effect of specialization on morphological and taxonomic diversity. Paleobiology 30:108–128.

Houle, D., G. H. Bolstad, K. van der Linde, and T. F. Hansen. 2017. Mutation predicts 40 million years of fly wing evolution. Nature 548:447–450.

Hubbe, A., D. Melo, and G. Marroig. 2016. A case study of extant and extinct Xenarthra cranium covariance structure: implications and applications to paleontology. Paleobiology 42:465–488.

Jablonski, D. 2019. Developmental bias, macroevolution, and the fossil record. Evolution and Development 22:103–125.

Jolicoeur, P. 1963. The multivariate generalization of the allometry equation. Biometrics 19:497–499.

Kissling, W. D., L. Dalby, C. Fløjgaard, J. Lenoir, B. Sandel, C. Sandom, K. Trøjelsgaard, et al. 2014. Establishing macroecological trait datasets: digitalization, extrapolation, and validation of diet preferences in terrestrial mammals worldwide. Ecology and Evolution 4:2913–2930.

Koepfli, K.-P., J. Pollinger, R. Godinho, J. Robinson, A. Lea, S. Hendricks, R. M. Schweizer, et al. 2015. Genome-wide evidence reveals that African and Eurasian golden jackals are distinct species. Current biology 25:2158–2165.

Kohn, L., and W. Atchley. 1988. How similar are genetic correlation structures data from mice and rats. Evolution 42:467–481.

Koyabu, D. D., W. W. Maier, and M. R. M. Sánchez-Villagra. 2012. Paleontological and developmental evidence resolve the homology and dual embryonic origin of a mammalian skull bone, the interparietal. Proceedings of the National Academy of Sciences of the USA 109:14075–14080.

Lande, R. 1979. Quantitative genetic analysis of multivariate evolution, applied to brain : body size allometry. Evolution 33:402–416.

Lofsvold, D. 1986. Quantitative genetics of morphological differentiation in *Peromyscus*. I. Tests of the homogeneity of genetic covariance structure among species and subspecies. Evolution 40:559–573.

———. 1988. Quantitative genetics of morphological differentiation in *Peromyscus*. II. Analysis of selection and drift. Evolution 42:54–67.

Lucherini, M., and E. M. Luengos Vidal. 2008. *Lycalopex gymnocercus* (Carnivora: Canidae). Mammalian Species 820:1–9.

Machado, F. A. 2020. Data from: Selection and constraints in the ecomorphological adaptive evolution of the skull of living Canidae (Carnivora, Mammalia). American Naturalist, Dryad Digital Repository, https://doi.org/10.5061/dryad.m63xsj3z9.

Machado, F. A., A. Hubbe, D. Melo, A. Porto, and G. Marroig. 2019. Measuring the magnitude of morphological integration: the effect of differences in morphometric representations and the inclusion of size. Evolution 73:2518–2528.

Machado, F. A., and P. Teta. 2020. Morphometric analysis of skull shape reveals unprecedented diversity of African Canidae. Journal of Mammalogy 101:349–360.

Machado, F. A., T. M. G. Zahn, and G. Marroig. 2018. Evolution of morphological integration in the skull of Carnivora (Mammalia): changes in Canidae lead to increased evolutionary potential of facial traits. Evolution 72:1399–1419.

Marroig, G., and J. M. Cheverud. 2001. A comparison of phenotypic variation and covariation patterns and the role of phylogeny, ecology, and ontogeny during cranial evolution of New World monkeys. Evolution 55:2576–2600.

———. 2004. Did natural selection or genetic drift produce the cranial diversification of Neotropical monkeys? American Naturalist 163:417–428.

———. 2005. Size as a line of least evolutionary resistance: diet and adaptive morphological radiation in new world monkeys. Evolution 59:1128–1142.

———. 2010. Size as a line of least resistance. II. Direct selection on size or correlated response due to constraints? Evolution 64:1470–1488.

Marroig, G., D. A. R. Melo, and G. R. G. Garcia. 2012. Modularity, noise, and natural selection. Evolution 66:1506–1524.

Marroig, G., L. T. Shirai, A. Porto, F. B. de Oliveira, and V. Conto. 2009. The evolution of modularity in the mammalian skull. II. Evolutionary consequences. Evolutionary Biology 36:136–148.

Maynard Smith, J., R. Burian, S. Kauffman, P. Alberch, J. Campbell, B. Goodwin, R. Lande, D. Raup, and L. Wolpert. 1985. Developmental constraints and evolution: a perspective from the Mountain Lake Conference on Development and Evolution. Quarterly Review of Biology 60:265–287.

McGlothlin, J. W., M. E. Kobiela, H. V. Wright, D. L. Mahler, J. J. Kolbe, J. B. Losos, and E. D. Brodie III. 2018. Adaptive radiation along a deeply conserved genetic line of least resistance in *Anolis* lizards. Evolution Letters 112:21–13.

Mech, L. D. 1974. *Canis lupus*. Mammalian Species 37:1–6.

Melo, D., A. Porto, and J. M. Cheverud. 2016. Modularity: genes, development, and evolution. Annual Review of Ecology, Evolution, and Systematics 47:463–486.

Meloro, C., A. Hudson, and L. Rook. 2014. Feeding habits of extant and fossil canids as determined by their skull geometry. Journal of Zoology 295:178–188.

Merkle, E. C., and Y. Rosseel. 2018. blavaan: Bayesian structural equation models via parameter expansion. Journal of Statistical Software 85:1–30.

Michaud, M., G. Veron, S. Peigné, A. Blin, and A. C. Fabre. 2018. Are phenotypic disparity and rate of morphological evolution correlated with ecological diversity in Carnivora? Biological Journal of the Linnean Society 124:294–307.

Mitteroecker, P., and F. Bookstein. 2011. Linear discrimination, ordination, and the visualization of selection gradients in modern morphometrics. Evolutionary Biology 38:100–114.

Moehlman, P. D., and V. Hayssen. 2018. *Canis aureus* (Carnivore: Canidae). Mammalian Species 50:14–25.

Myers, P., R. Espinosa, C. S. Parr, T. Jones, G. S. Hammond, and T. A. Dewey. 2018. The Animal Diversity Web. https://animaldiversity.org.

Nogueira, M. R., A. L. Peracchi, and L. R. Monteiro. 2009. Morphological correlates of bite force and diet in the skull and mandible of phyllostomid bats. Functional Ecology 23:715–723.

Penrose, F., G. J. Kemp, and N. Jeffery. 2016. Scaling and accommodation of jaw adductor muscles in Canidae. Anatomical 299:951–966.

Phillips, A. G., T. Töpfer, C. Rahbek, K. Böhning-Gaese, and S. A. Fritz. 2018. Effects of phylogeny and geography on ecomorphological traits in passerine bird clades. Journal of Biogeography 45:2337–2347.

Pilatti, P., and D. Astúa. 2017. Orbit orientation in didelphid marsupials (Didelphimorphia: Didelphidae). Current Zoology 63:403–415.

Piras, P., D. Silvestro, F. Carotenuto, S. Castiglione, A. Kotsakis, L. Maiorino, M. Melchionna, et al. 2018. Evolution of the sabertooth mandible: a deadly ecomorphological specialization. Palaeogeography, Palaeoclimatology, Palaeoecology 496:166–174.

Radinsky, L. B. 1981. Evolution of skull shape in carnivores. 1. Representative modern carnivores. Biological Journal of the Linnean Society 15:369–388.

Renaud, S., J.-C. Auffray, and J. Michaux. 2006. Conserved phenotypic variation patterns, evolution along lines of least resistance, and departure due to selection in fossil rodents. Evolution 60:1701–1717.

Revell, L. J., L. J. Harmon, R. B. Langerhans, and J. J. Kolbe. 2007. A phylogenetic approach to determining the importance of constraint on phenotypic evolution in the Neotropical lizard *Anolis cristatellus*. Evolutionary Ecology Research 9:261–282.

Roff, D. A. 1995. The estimation of genetic correlations from phenotypic correlations: a test of Cheverud's conjecture. Heredity 74:481–490.

Rosseel, Y. 2012. lavaan: an R package for structural equation modeling. Journal of Statistical Software 48:1–36.

Rutledge, Linda Y. 2010. Evolutionary origins, social structure, and hybridization of the eastern wolf, *Canis lycaon*. Thesis. Trent University, Peterborough, Ontario.

Schluter, D. 1996. Adaptive radiation along genetic lines of least resistance. Evolution 50:1766–1774.

Schoch, R. R. 2006. Skull ontogeny: developmental patterns of fishes conserved across major tetrapod clades. Evolution and Development 8:524–536.

Segura, V., G. H. Cassini, F. J. Prevosti, and F. A. Machado. 2020. Integration or modularity in the mandible of canids (Carnivora: Canidae): a geometric morphometric approach. Journal of Mammalian Evolution (forthcoming), http://doi.org/10.1007/s10914-020-09502-z.

Sillero-Zubiri, C., and D. Gottelli. 1994. *Canis simensis*. Mammalian Species 485:1–6.

Sillero-Zubiri, C., M. Hoffmann, and D. W. Macdonald. 2004. Canids: foxes, wolves, jackals, and dogs: status survey and conservation action plan. IUCN, Gland.

Simon, M. N., F. A. Machado, and G. Marroig. 2016. High evolutionary constraints limited adaptive responses to past climate changes in toad skulls. Proceedings of the Royal Society B 283:20161783.

Slater, G. J. 2015. Iterative adaptive radiations of fossil canids show no evidence for diversity-dependent trait evolution. Proceedings of the National Academy of Sciences of the USA 112:4897–4902.

Slater, G. J., E. R. Dumont, and B. Van Valkenburgh. 2009. Implications of predatory specialization for cranial form and function in canids. Journal of Zoology 278:181–188.

Spencer, M. A. 1998. Force production in the primate masticatory system: electromyographic tests of biomechanical hypotheses. Journal of Human Evolution 34:25–54.

Tastle, W., and M. Wierman. 2007. Consensus and dissention: a measure of ordinal dispersion. International Journal of Approximate Reasoning 45:531–545.

Tedford, R. H., X. Wang, and B. E. Taylor. 2009. Phylogenetic systematics of the North American fossil Caninae (Carnivora: Canidae). Bulletin of the American Museum of Natural History 325:1–218.

Therrien, F. 2005. Mandibular force profiles of extant carnivorans and implications for the feeding behaviour of extinct predators. Journal of Zoology 267:249–270.

Therrien, F., A. Quinney, K. Tanaka, and D. K. Zelenitsky. 2016. Accuracy of mandibular force profiles for bite force estimation and feeding behavior reconstruction in extant and extinct carnivorans. Journal of Experimental Biology 219:3738–3749.

Tucker, M. A., T. J. Ord, and T. L. Rogers. 2016. Revisiting the cost of carnivory in mammals. Journal of Evolutionary Biology 29:2181–2190.

Turelli, M. 1988. Phenotypic evolution, constant covariances, and the maintenance of additive variance. Evolution 42:1342–1347.

Van Valkenburgh, B. 1988. Trophic diversity in past and present guilds of large predatory mammals. Paleobiology 14:155–173.

———. 1991. Iterative evolution of hypercarnivory in canids (Mammalia: Carnivora): evolutionary interactions among sympatric predators. Paleobiology 17:340–362.

———. 2007. Deja vu: the evolution of feeding morphologies in the Carnivora. American Zoologist 47:47–163.

Van Valkenburgh, B., and K. Koepfli 1993. Cranial and dental adaptations to predation in canids. Symposium of the Zoological Society of London 65:15–37.

Van Valkenburgh, B., X. Wang, and J. Damuth. 2004. Cope's rule, hypercarnivory, and extinction in North American canids. Science 306:101–104.

Van Valkenburgh, B., and R. K. Wayne. 1994. Shape divergence associated with size convergence in sympatric East African jackals. Ecology 75:1567–1581.

Vézina, A. F. 1985. Empirical relationships between predator and prey size among terrestrial vertebrate predators. Oecologia 67:555–565.

Villmoare, B. 2013. Morphological integration, evolutionary constraints, and extinction: a computer simulation-based study. Evolutionary Biology 40:76–83.

Wang, X. 1994. Phylogenetic systematics of the Hesperocyoninae (Carnivora, Canidae). Bulletin of the American Museum of Natural History 221:1–207.

Wang, X., R. H. Tedford, and B. E. Taylor. 1999. Phylogenetic systematics of the Borophaginae (Carnivora, Canidae). Bulletin of the American Museum of Natural History 243:1–391.

Wayne, R. 1986. Cranial morphology of domestic and wild canids: the influence of development on morphological change. Evolution 40:243–261.

Werdelin, L. 1989. Constraint and adaptation in the bone-cracking canid *Osteoborus* (Mammalia: Canidae). Paleobiology 15:387–401.

Werdelin, L., and G. D. Wesley-Hunt. 2014. Carnivoran ecomorphology: patterns below the family level. Annales Zoologici Fennici 51:259–268.

Zrzavý, J., P. Duda, J. Robovský, I. Okřinová, and V. P. Řičánková. 2018. Phylogeny of the Caninae (Carnivora): combining morphology, behaviour, genes and fossils. Zoologica Scripta 47:373–389.

Zurano, J. P., P. A. Martinez, J. Canto-Hernandez, J. I. Montoya-Burgos, and G. C. Costa. 2017. Morphological and ecological divergence in South American canids. Journal of Biogeography 44:821–833.

## References Cited Only in the Online Enhancements

Arnold, C., L. J. Matthews, and C. L. Nunn. 2010. The 10kTrees website: a new online resource for primate phylogeny. Evolutionary Anthropology 19:114–118.

Atickem, A., N. C. Stenseth, M. Drouilly, S. Bock, C. Roos, and D. Zinner. 2017. Deep divergence among mitochondrial lineages in African jackals. Zoologica Scripta 47:1–8.

Cardini, A. 2019. Integration and modularity in Procrustes shape data: is there a risk of spurious results? Evolutionary Biology 46:90–105.

Chetri, M., Y. Jhala, S. R. Jnawali, N. Subedi, M. Dhakal, and B. Yumnam. 2016. Ancient Himalayan wolf (*Canis lupus chanco*) lineage in Upper Mustang of the Annapurna Conservation Area, Nepal. ZooKeys 582:143–156.

Cheverud, J. M. 1982. Phenotypic, genetic, and environmental morphological integration in the cranium. *Evolution* 36:499–516.

Linde, K., and D. Houle. 2009. Inferring the nature of allometry from geometric data. Evolutionary Biology 36:311–322.

Melo, D., G. R. G. Garcia, A. Hubbe, A. P. Assis, and G. Marroig. 2015. EvolQG: an R package for evolutionary quantitative genetics. F1000Research 4:1–9.

Paradis, E., J. Claude, and K. Strimmer. 2004. APE: analyses of phylogenetics and evolution in R language. Bioinformatics 20:289–290.

Perini, F., C. A. M. Russo, and C. Schrago. 2010. The evolution of South American endemic canids: a history of rapid diversification and morphological parallelism. Journal of Evolutionary Biology 23:311–322.

Rueness, E. K., M. G. Asmyhr, C. Sillero-Zubiri, D. W. Macdonald, A. Bekele, A. Atickem, and N. C. Stenseth. 2011. The cryptic African wolf: *Canis aureus lupaster* is not a golden jackal and is not endemic to Egypt. PLOS ONE 6:e16385.

Schliep, K. P. 2011. phangorn: phylogenetic analysis in R. Bioinformatics 27:592–593.

Slater, G. J., L. J. Harmon, and M. E. Alfaro. 2012. Integrating fossils with molecular phylogenies improves inference of trait evolution. Evolution 66:3931–3944.

Theobald, D. L. 2006. THESEUS: maximum likelihood superpositioning and analysis of macromolecular structures. Bioinformatics 22:2171–2172.

Torcida, S., S. Ivan Perez, and P. N. Gonzalez. 2013. An integrated approach for landmark-based resistant shape analysis in 3D. Evolutionary Biology 41:351–366.

Viranta, S., A. Atickem, L. Werdelin, and N. C. Stenseth. 2017. Rediscovering a forgotten canid species. BMC Zoology 2:1–9.

Vonholdt, B. M., J. A. Cahill, Z. Fan, I. Gronau, J. Robinson, J. P. Pollinger, B. Shapiro, J. Wall, and R. K. Wayne. 2016. Whole-genome sequence analysis shows that two endemic species of North American wolf are admixtures of the coyote and gray wolf. Science Advances 2:e1501714.

Walker, J. A. 2000. Ability of geometric morphometric methods to estimate a known covariance matrix. Systematic Zoology 49:686–696.

Weaver, T. D., and P. Gunz. 2018. Using geometric morphometric visualizations of directional selection gradients to investigate morphological differentiation. Evolution 72:838–850.

Werhahn, G., H. Senn, J. Kaden, J. Joshi, S. Bhattarai, N. Kusi, C. Sillero-Zubiri, and D. W. Macdonald. 2017. Phylogenetic evidence for the ancient Himalayan wolf: towards a clarification of its taxonomic status based on genetic sampling from western Nepal. Royal Society Open Science 4:170186.

Zrzavý, J., and V. Ricankova. 2004. Phylogeny of recent Canidae (Mammalia, Carnivora): relative reliability and utility of morphological and molecular datasets. Zoologica Scripta 33:311–333.

Associate Editor: Scott J. Steppan
Editor: Russell Bonduriansky